Neutron total scattering and reverse Monte Carlo study of cation ordering in $Ca_xSr_{1-x}TiO_3$

2007 J. Phys.: Condens. Matter 19 335214

(http://iopscience.iop.org/0953-8984/19/33/335214)

IOP PUBLISHING JOURNAL OF PHYSICS: CONDENSED MATTER

J. Phys.: Condens. Matter **19** (2007) 335214 (11pp) doi:10.1088/0953-8984/19/33/335214

Neutron total scattering and reverse Monte Carlo study of cation ordering in $Ca_xSr_{1-x}TiO_3$

Qun Hui[1,3], Martin T Dove[1,4], Matthew G Tucker[1,2], Simon A T Redfern[1] and David A Keen[2]

[1] Department of Earth Sciences, University of Cambridge, Downing Street, Cambridge CB2 3EQ, UK
[2] ISIS Facility, Rutherford Appleton Laboratory, Chilton, Didcot, Oxfordshire OX11 0QX, UK

E-mail: mtd10@cam.ac.uk

Received 3 May 2007
Published 4 July 2007
Online at stacks.iop.org/JPhysCM/19/335214

Abstract

We use neutron total scattering measurements with reverse Monte Carlo analysis methods incorporating an atom-swapping algorithm to identify the short-range Ca/Sr cation ordering within the $Ca_xSr_{1-x}TiO_3$ solid solution (compositions $x = 0.2, 0.5, 0.8$). Our results show that nearest-neighbour pairs have a strong tendency for unlike Ca/Sr first-neighbour coordination in the $x = 0.2$ and 0.5 cases. In the $x = 0.5$ case the Ca/Sr ordering results in a structure with space group $P2_1nm$. In contrast, there is much less short-range cation ordering in the $x = 0.8$ case.

(Some figures in this article are in colour only in the electronic version)

1. Introduction

The crystal structures of the various phases within the $Ca_xSr_{1-x}TiO_3$ perovskite solid solution have been the objects of many investigations in recent years. Much of this work has been summarized and reviewed by Carpenter *et al* [1]. The phase behaviour of the two end-member phases is well understood. The $x = 0$ end member, $SrTiO_3$, has the ideal cubic perovskite structure at room temperature, with a transition at 105 K to the tetragonal space group $I4/mcm$, involving a small rotation of the TiO_6 octahedra about a single axis. The $x = 1$ end member, $CaTiO_3$, has a more distorted structure at room temperature, with separate rotations of the TiO_6 octahedra about each of the three crystallographic axes. The crystal structure of this phase is orthorhombic, with space group $Pnma$. The phase transitions in $CaTiO_3$ occur on heating. The first transition is to the same tetragonal structure of $SrTiO_3$ at a temperature of 1498 ± 24 K,

[3] Present address: School of Material Science and Engineering, Southwest University, Chongqing 400715, People's Republic of China.
[4] Author to whom any correspondence should be addressed.

and second to the cubic phase at 1634 ± 13 K [2, 3]. Carpenter *et al* [1] performed new high-resolution neutron diffraction measurements to determine a detailed phase diagram over the full range of compositions and temperatures from 4.2 K to in excess of 1600 K. At room temperature, the structures are reported to have space groups $Pnma$ for $1 > x < 0.41$, $Pbcm$ for $0.41 > x > 0.37$, $I4/mcm$ for $0.37 > x > 0.07$ and $Pm\bar{3}m$ for $0.07 > x > 0$. Previous work had suggested the possibilities of phases of other symmetries with varying composition, but the results of Carpenter *et al* [1] now appear to rule these out.

The crystallographic work to date appears to have not considered the possibility of ordering of the Ca and Sr cations on the perovskite crystallographic **A** sites, i.e. the cation sites with 12-fold coordination with respect to the oxygen atoms. Our own Rietveld refinements (see below) suggest that any cation ordering is extremely difficult to detect through standard powder diffraction methods. In this paper we investigate cation ordering for three members of the $Ca_xSr_{1-x}TiO_3$ solid solution, $x = 0.2, 0.5, 0.8$, at ambient temperature using neutron total scattering analysed using the reverse Monte Carlo (RMC) method. Neutron total scattering provides information about the pair distribution function, which should in turn provide a new source of data concerning cation ordering. We propose that this approach may be useful for materials that exhibit atomic order and where information about the ordering is hard to extract from the Bragg peaks in the powder diffraction data alone. Anticipating the results reported here, we will find that there is significant cation ordering for two of the three examples we have studied, and we are able to propose a long-range ordered structure for the stoichiometric composition $Ca_{0.5}Sr_{0.5}TiO_3$. In addition to providing new crystallographic information about this material, this paper reports the first case study of the 'atom-swapping' algorithm implemented within the `RMCProfile` program for crystalline materials [4] (see references [5–10] for previous related methods).

2. Experimental and analysis methods

The samples used in this work were synthesized by drying $CaCO_3$ (Chempur, 99.9%) and $SrCO_3$ (Aldrich, 99.999%) at 500 °C and TiO_2 (Aldrich, 99.9%) at 1000 °C for 3 h. Mixtures of stoichiometric amounts were heated to 1300 °C at a rate of 20 °C h^{-1} and kept at that temperature for 4 h. After grinding in an agate mortar and pressing into pellets, the samples were fired in air at 1600 °C for 48 h with periodic regrinding and repressing. Analysis by microprobe showed that all samples are close to the nominal compositions and homogeneous at the 1% level.

Neutron diffraction measurements were performed on the GEM diffractometer at the ISIS pulsed spallation neutron source [11]. The sample was contained in a cylindrical vanadium can with internal diameter of 0.8 cm and height of 4 cm. Data were collected under ambient conditions taking 6 h per sample. Time was also given for background correction and calibration runs. Standard methods were used to correct the data for analysis as total scattering data, using the approach described previously [12]. Data from the full set of detector banks were merged (with a range of values of Q of 0.6–46 $Å^{-1}$) and Fourier transformed to produce the pair distribution function $D(r)$; the case for $x = 0.5$ is shown in figure 1.

We make one comment in passing. For RMC studies from total scattering, the highest maximum value of Q possible is recommended in order to obtained the best possible resolution in real space. This is particularly important when studying thermal fluctuations, for example. In the case of using the RMC method to study cation ordering, we envisage (although without having quantified this) that in fact a high maximum value of Q is less important, because the critical quantity for the determination of short-range correlations is the integrals of the near-neighbour peaks in the pair distribution function rather than the shapes of the peaks. On the

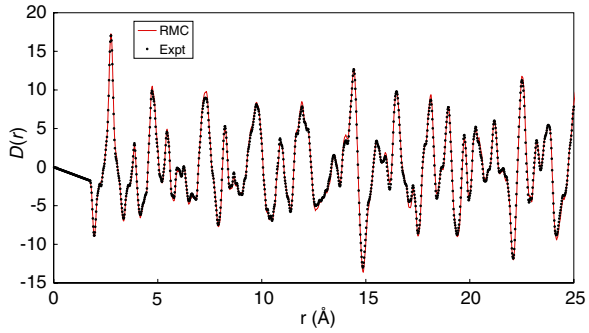

Figure 1. The pair distribution function $D(r)$ for $Ca_{0.5}Sr_{0.5}TiO_3$. The points represent the function obtained by transformation from the experimental neutron total scattering function, and the continuous curve represents the calculation from the RMC configuration.

other hand, the resolution obtainable with high Q will be useful for obtaining information about distortions to local atomic coordination due to the effects of the strain arising from different cation sizes.

Rietveld refinement was carried out using the GSAS software [13, 14]. Each refinement includes four banks of GEM data which were collected from low angles to high angles. In each refinement, the background coefficients, histogram scale factors, parameters for peak shapes, lattice parameters, atomic coordinates, isotropic thermal parameters and Ca/Sr site occupancy parameters were varied.

The general RMC analysis method for crystalline materials, as encapsulated within our program `RMCProfile`, has been described in detail elsewhere [12, 4]. Our approach is to use both the total scattering data in Q-space and the pair distribution function in r-space, and also to make explicit use of the Bragg diffraction data [15]. The benefit of separately handling the Bragg scattering is to directly include the information about long-range order contained in the Bragg peaks as distinct from the information about shorter-range atomic correlations contained within the total scattering data in the RMC analysis. We also used data-based restraints on the Ti–O distance and on the O–Ti–O angles to prevent atoms moving away from their equilibrium positions.

In each case, the dimensions of the RMC configurations were defined by the lattice parameters obtained from a prior Rietveld analysis performed using random site occupancies for the Ca and Sr atoms (results presented below). Our configurations consisted of 14 000 atoms corresponding to a $10 \times 10 \times 7$ supercell of the orthorhombic structure with approximate dimensions $55 \times 55 \times 54$ Å^3.

The atom-swapping method used in the `RMCProfile` code [4] involves alternating between swapping individual pairs of atoms and a set of displacement moves. The idea is that by modelling the pair distribution function, the RMC will generate configurations with the correct short-range cation site ordering. Coupled with the information on long-range ordering contained in the Bragg scattering data, the RMC method should provide a complete picture of the cation ordering within the configurations.

The example of Ca/Sr ordering in $Ca_xSr_{1-x}TiO_3$ is particularly challenging as a case study of the atom-swapping method. The most important features of the pair distribution function are the peaks for neighbouring **A** sites. Unfortunately, the simplicity of the perovskite structure means that these peaks overlap with Ti–Ti and O–O peaks. This point is quantified in appendix A, where we show that the effect of ordering on the pair distribution function will be of order $\pm 1\%$ on the integrated weights of the relevant peaks. The other effect of ordering on

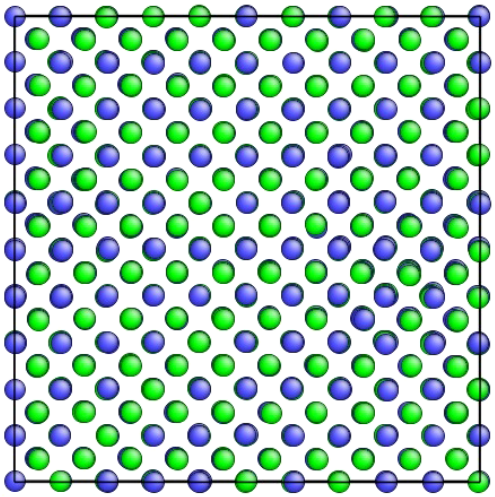

Figure 2. Snapshot of one of the RMC configurations of $Ca_{0.5}Sr_{0.5}TiO_3$, showing only the Ca and Sr cations. The rock salt ordering is apparent from this image.

$D(r)$ will be changes to the widths of peaks associated with the different sizes of the ordering cations.

Since this is the first case study performed using the atom-swapping algorithm in `RMCProfile` [4], we took particular care to ensure that the final results were not biased by the starting structure. Thus for the case of $Ca_{0.5}Sr_{0.5}TiO_3$ we used initial configurations with very different Ca/Sr site distributions. These included various different ordered states, completely random states, and states in which we distributed all of the Ca cations in one half of the configuration and all the Sr cations in the other half. All results converged to the same ordered pattern, confirming that the final result was not biased by the starting configuration. We also ran the simulations without the use of data to ensure that the basic Monte Carlo method was not itself giving biased results; this gave very different results (essentially random distributions).

3. Results

3.1. RMC analysis of Ca/Sr ordering in $Ca_{0.5}Sr_{0.5}TiO_3$

The comparison between the experimental and RMC-fitted pair distribution function $D(r)$ for $Ca_{0.5}Sr_{0.5}TiO_3$ is shown in figure 1; it can be seen that the RMC simulation has achieved a very good reproduction of the experimental data, which is essential if we are to see the effects of Ca/Sr ordering. A view of one of the resultant configurations of Ca and Sr cations is shown in figure 2. This shows the establishment of a rock salt ordering, with Ca cations being mostly coordinated by Sr cations and vice versa. This is the type of ordering that one might expect, with like cations avoiding being nearest neighbours. Presumably this ordering is driven by short-range strain interactions associated with the different sizes of the two cations. We noted above that we tested this result very thoroughly by making many repeated runs with different starting configurations; as a result we believe that it is a robust result. We will see below that this ordering pattern can be confirmed by Rietveld analysis.

The degree of short-range order is quantified by computing the function $n_{ij}(r)$, defined as the average number of atoms of type j lying within a sphere of radius r surrounding a central

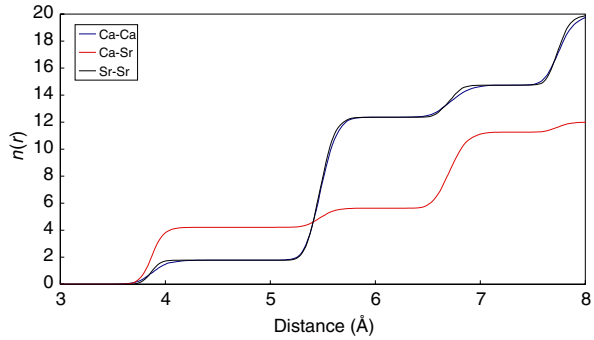

Figure 3. The function $n(r)$ for Ca and Sr atoms for $Ca_{0.5}Sr_{0.5}TiO_3$.

Table 1. Neighbour correlations from the RMC $n_{Ca-Ca}(r)$ data for $Ca_{0.5}Sr_{0.5}TiO_3$. The vector denotes the separation between sites with site coordination number; n_{Ca-Ca} is the number of Ca–Ca neighbours for each case, with a comparison of the results from the RMC simulation with the expected numbers for ordered and disordered configurations; α is the Warren–Cowley order parameter defined in appendix B.

Neighbour	Vector	Coordination	n^{RMC}_{Ca-Ca}	$n^{Ord.}_{Ca-Ca}$	$n^{Disord.}_{Ca-Ca}$	α
1	[100]	6	1.8	0	3	−0.41
2	[110]	12	10.6	12	6	0.77
3	[111]	8	2.4	0	4	−0.41

atom of type i. $n_{ij}(r)$ is shown for Ca and Sr pairs in figure 3. The coordination numbers obtained from the $n(r)$ data are give in table 1 and compared with the values for fully ordered and randomly disordered models; the comparison shows that the average coordination numbers are close to the values for complete ordering. We note that the pair distributions of two cations are highly constrained, with the values of $n_{Ca-Ca}(r)$, $n_{Ca-Sr}(r)$ and $n_{Sr-Sr}(r)$ being completely dependent on each other; this is discussed in appendix B.

The analysis of the RMC configurations shows that the crystal structure has the structure shown in figure 4, with space group $P2_1nm$.

3.2. RMC analysis of Ca/Sr ordering in $Ca_xSr_{1-x}TiO_3$, $x = 0.2, 0.8$

We have repeated our analysis for the two non-stoichiometric materials. The $n(r)$ analyses are shown in figure 5 and the key results are summarized in table 2. In table 2 we compare the RMC results with two possible models, one in which we have complete disorder of two Ca and Sr cations on the perovskite **A** sites, and the other based on a rock salt ordering as seen in the $x = 0.5$ case. In the latter case, we can define two subsets of the **A** sites with the rock salt arrangement: **A1** which is preferentially occupied by Ca and **A2** which is preferentially occupied by Sr. For $x = 0.2$, we assume that the ordered state is described with **A2** sites that are 100% occupied by Sr, and **A1** sites that have 40% occupancy by Ca and 60% occupancy by Sr with random arrangement of the Ca and Sr cations over the **A1** sites. For $x = 0.8$, we assume that the **A1** sites are 100% occupied by Ca, and the **A2** sites have 40% occupancy by Sr and 60% occupancy by Ca. We note that this ordering will probably not lead to long-range order because the proportions of the two types of cation are too different from 50:50, but this ordering might be expected to exist over the short distances encompassed by the first few neighbours. The point is that these are models of ordered states, and any actual ordering may

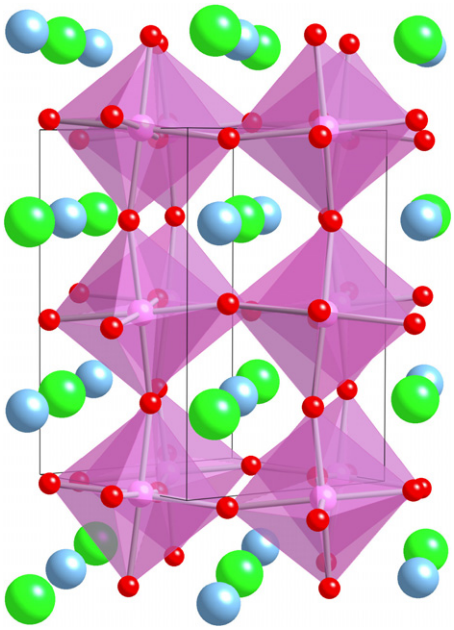

Figure 4. The proposed structure of $Ca_{0.5}Sr_{0.5}TiO_3$.

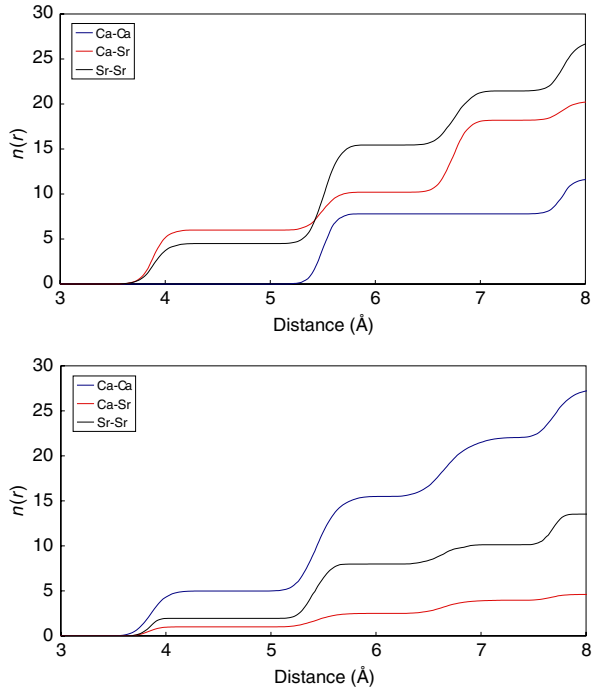

Figure 5. The $n(r)$ functions for $Ca_xSr_{1-x}TiO_3$, $x = 0.2$ (top) and $x = 0.8$ (bottom).

be different; the model given here provides a benchmark against which the RMC results can be evaluated.

Table 2. Neighbour correlations from the RMC $n(r)$ data for $Ca_xSr_{1-x}TiO_3$. The vector denotes the separation between sites with site coordination number; n_{Ca-Ca} is the number of Ca–Ca neighbours for each case, with a comparison of the results from the RMC simulation with the expected numbers for ordered and disordered configurations; α is the Warren–Cowley order parameter defined in appendix B. The ordered result is obtained by assuming a rock salt ordering pattern as described in the text.

x	Neighbour	Vector	Coordination	n^{RMC}_{Ca-Ca}	$n^{Ord.}_{Ca-Ca}$	$n^{Disord.}_{Ca-Ca}$	α
0.2	1	[100]	6	0.0	0	1.2	0.5
	2	[110]	12	7.8	4.8	2.4	0.83
	3	[111]	8	0	0	1.6	0.50
0.8	1	[100]	6	5.0	3.6	4.8	−0.33
	2	[110]	12	10.5	12	9.6	0
	3	[111]	8	6.5	3.2	6.4	−0.50

A number of points emerge from the data presented in table 2. For the case $x = 0.2$ the RMC configurations have complete avoidance of Ca $\cdots$ Ca first and third neighbours, as in the case of $x = 0.5$. However, the predictions of the ordered rock salt model with disorder over the **A** sites does not correctly describe the value of n^{RMC}_{Ca-Ca} for second neighbour. In fact, n^{RMC}_{Ca-Ca} for second neighbour is higher than predicted by both ordered and disordered models. One straightforward interpretation is that a rock salt Ca/Sr ordering is occurring, but that there are clusters that are richer in Ca content than predicted by the chemical composition, with concomitant Ca-deficient clusters.

On the other hand, for the case $x = 0.8$ the cation ordering is more consistent with a completely random arrangement of the Ca and Sr cations. In fact there is a slight increase of the value of the first-neighbour n^{RMC}_{Ca-Ca} over the random value (noting that in the hypothetical ordering the value of n_{Ca-Ca} will be lower than the value for random disorder), but this is not likely to be significant.

3.3. Rietveld refinements

With the predicted ordered structure of the $x = 0.5$ phase, we have performed new Rietveld refinements of the structure, together with refinements of the other two compositions. In each case we provided constraints on the isotropic temperature factors of the Ca and Sr cations. We adjusted the site occupancies in all refinements; this was in order to check that the resultant values are consistent with known compositions, so that we could then also trust the refined values for the one case (the ordered structure of the $x = 0.5$ phase) where we do not have an independent chemical check. Moreover, the check also provides us with independent information on the stabilities of the refinements in view of the common correlations between site occupancies and temperature factors.

The results of the Rietveld refinements are given in table 3. A representative fitted diffraction pattern is shown in figure 6.

From table 3 it is clear that the effect of ordering on the Rietveld fit on the R-factors is slight, and it would be hard to argue for the presence of ordering from the Bragg diffraction data alone. Thus the key evidence for cation ordering actually comes from the pair distribution functions obtained from the RMC analysis.

The refinement of the ordered $P2_1nm$ structure of the $x = 0.5$ composition allowed the site occupancies of the Ca/Sr sites to vary. The refined site occupancies for the ordered $P2_1nm$ structure of the $x = 0.5$ composition are consistent with a rock salt ordering pattern, with the values of the site occupancies of 80:20 per site are similar to the value of 85:15 obtained

Table 3. Results of Rietveld refinements for $Ca_xSr_{1-x}TiO_3$. Standard deviations on the last significant figures are given in brackets. We give results for two refinements for $x = 0.5$, one (space group $P2_1nm$) for a cation-ordered state and the other (space group $Pbnm$) for a cation-disordered state. Note that for space group $P2_1nm$ we use a setting with the origin on the 2_1 axis and in the plane of reflection of the n glide plane, with the mirror plane at height $z = 1/4$. (Note: the standard R factors for the structural refinements are $Ca_{0.5}Sr_{0.5}TiO_3$: $P2_1nm$: $R_p = 4.1\%$, $R_{wp} = 4.3\%$; $Ca_{0.5}Sr_{0.5}TiO_3$: $Pbnm$: $R_p = 4.2\%$, $R_{wp} = 4.3\%$; $Ca_{0.2}Sr_{0.8}TiO_3$: $R_p = 3.7\%$, $R_{wp} = 3.8\%$; $Ca_{0.8}Sr_{0.2}TiO_3$: $R_p = 4.6\%$, $R_{wp} = 4.2\%$).

Atom	Occupancy	x	y	z	U_{iso} (Å^2)
$Ca_{0.5}Sr_{0.5}TiO_3$: $P2_1nm$, $a = 5.4727(2)$, $b = 5.4731(1)$, $c = 7.7326(2)$ Å					
Ca1	0.79(2)	−0.017(1)	0.268(1)	1/4	0.59(2)
Ca2	0.21(2)	0.483(1)	0.756(1)	1/4	0.59(2)
Sr1	0.21(2)	−0.017(1)	0.268(1)	1/4	0.59(2)
Sr2	0.79(2)	0.483(1)	0.756(1)	1/4	0.59(2)
Ti	1	0	0.751(1)	0.0033(9)	0.59(3)
O1	1	−0.050(1)	0.747(1)	1/4	0.99(1)
O2	1	0.213(1)	0.0306(5)	0.0280(4)	0.99(1)
O3	1	0.046(1)	0.7588(8)	3/4	0.99(1)
O4	1	0.761(1)	0.4851(4)	−0.0230(3)	0.99(1)
$Ca_{0.5}Sr_{0.5}TiO_3$: $Pbnm$, $a = 5.4722(2)$, $b = 5.4736(2)$, $c = 7.7327(2)$ Å					
Ca	0.503(6)	0.0028(5)	0.5131(2)	1/4	0.73(1)
Sr	0.497(6)	0.0026(5)	0.5131(2)	1/4	0.73(1)
Ti	1	0	0	0	0.60(1)
O1	1	−0.0536(2)	−0.0057(3)	1/4	0.94(2)
O2	1	0.2272(1)	0.2722(2)	0.0232(1)	0.93(1)
$Ca_{0.8}Sr_{0.2}TiO_3$: $Pbnm$, $a = 5.420\,53(6)$, $b = 5.449\,42(6)$, $c = 7.682\,10(9)$ Å					
Ca	0.826(6)	0.0048(2)	0.5255(1)	1/4	0.91(2)
Sr	0.174(6)	0.0048(2)	0.5255(1)	1/4	0.91(2)
Ti	1	0	0	0	0.62(1)
O1	1	−0.063(2) (1)	−0.0120(1)	1/4	0.94(1)
O2	1	0.2157(1)	0.2847(1)	0.0324(1)	0.98(1)
$Ca_{0.2}Sr_{0.8}TiO_3$: $I4/mcm$, $a = b = 5.500\,97(3)$, $c = 7.805\,9(8)$ Å					
Ca	0.189(6)	0	1/2	1/4	0.77(1)
Sr	0.811(6)	0	1/2	1/4	0.77(1)
Ti	1	0	0	0	0.50(1)
O1	1	0	0	1/4	1.15(2)
O2	1	0.770 82(5)	0.270 82(5)	0	0.98(1)

directly from the RMC configurations. We note from table 3 that there is good consistency in general between refined site occupancies with chemical composition, and that the temperature factors are consistent between different compositions.

4. Conclusion and discussion

In this paper we have shown how RMC methods with an atom-swapping algorithm can be used to obtain information about the long-range and short-range Ca/Sr cation ordering in the perovskite $Ca_xSr_{1-x}TiO_3$. The interesting point is that only a small effect on the pair distribution function can create order within the RMC configurations.

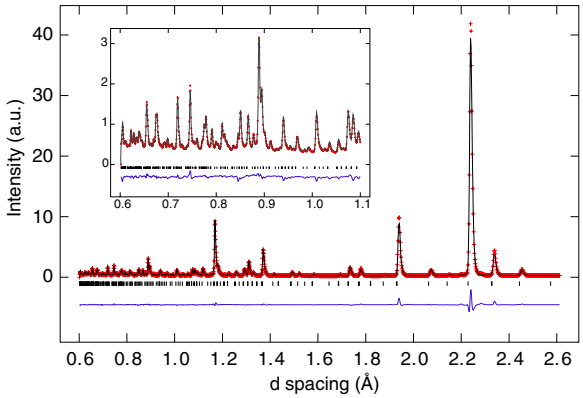

Figure 6. The Rietveld-fitted diffraction pattern for $Ca_{0.5}Sr_{0.5}TiO_3$ in space group $P2_1nm$.

What is happening within the RMC is that a degree of long-range order is generated to a large part through the short-range order imposed by the information contained within the pair distribution function; at least, that is what is suggested by the fact that the disordered structure gives a fit to the diffraction pattern that is almost as good as the ordered structure. We need to consider under which circumstances we might be able to use this approach to determine the long-range ordered structure. To address this issue, we can use our work on cation ordering using pair potentials. In the case of equal numbers of ordering cations, a high degree of short-range order will necessarily force the configurations to have long-range order. Within a mean-field approximation (MFA), there is a direct correlation between the site order and the numbers of nearest neighbours. Specifically, for a site with z neighbours and containing y **A** cations and $1 - y$ **B** cations (where **A** and **B** are identified as Ca and Sr in the present case, and $z = 6$ for nearest neighbours in the perovskite structure), the MFA would predict that the number of $A \cdots B$ neighbours is

$$n_{\mathbf{A}\cdots\mathbf{B}} = zy^2. \tag{1}$$

However, the MFA is not valid for cation-ordering phase transitions, and Monte Carlo simulations of ordering processes using pair potentials show that configurations can accommodate a high degree of short-range order before forcing the system to develop long-range order. Thus the values of site occupancies will always be lower than implied by the MFA, so we have the inequality

$$y < (n_{\mathbf{A}\cdots\mathbf{B}}/z)^{1/2}. \tag{2}$$

For the case of equal numbers of cations on a cubic lattice with NaCl ordering (as in the case of $Ca_{0.5}Sr_{0.5}TiO_3$) and nearest-neighbour interactions, Monte Carlo simulations suggest that long-range ordering occurs when $y \sim 0.72$, although this condition will be dependent on details of the structure (number of neighbours etc). Comparing the Rietveld refinements with the values of $n^{\mathrm{RMC}}_{\mathrm{Ca-Ca}}$ for $x = 0.5$, the site occupancy value of 0.8 lies between the bounds of 0.72 from the Monte Carlo simulation and the value of $(n/z)^{1/2}$.

In cases where there is an unequal number of ordering cations, the failure of the MFA is even worse, and typically when the ratio of the two cations approaches 1:2 the short-range order is never sufficient to drive long-range order. Thus in these cases the analysis will rely on the information content within the Bragg diffraction pattern to predict the existence of long-range order. That said, it is often the case that such cases do not actually order, in which case the issue

of predicting long-range order does not occur. This is the case for our examples with $x = 0.2$ and 0.8.

Acknowledgment

We acknowledge funding from Engineering and Physical Sciences Research Council (EPSRC).

Appendix A. Quantifying the effect of cation ordering on the peaks in $D(r)$

The total distribution function $D(r)$ function is expressed as

$$D(r) = 4\pi\rho r \sum_{j,k=1}^{n} c_j c_k \bar{b}_j \bar{b}_k \left(g_{jk}(r) - 1\right) \tag{A.1}$$

where the partial functions, $g_{jk}(r)$ are normalized such that $g_{jk}(r \to \infty) = 1$, c_j is the number concentration of atomic species j, and $\bar{b}_j$ is the coherent neutron scattering length of atom j. From the chemical formula, the atom concentrations are $c_{\mathrm{Ca}} = c_{\mathrm{Sr}} = 0.1$, $c_{\mathrm{O}} = 0.6$ and $c_{\mathrm{Ti}} = 0.2$. The neutron scattering length for each atom is $\bar{b}_{\mathrm{Ca}} = 4.70$ fm, $\bar{b}_{\mathrm{Sr}} = 7.02$ fm, $\bar{b}_{\mathrm{Ti}} = -3.44$ fm and $\bar{b}_{\mathrm{O}} = 5.80$ fm. In the disordered cation configuration for $Ca_{0.5}Sr_{0.5}TiO_3$, the partial distribution functions $g_{\mathrm{CaCa}}(r)$, $g_{\mathrm{CaSr}}(r)$, $g_{\mathrm{SrCa}}(r)$ and $g_{\mathrm{SrSr}}(r)$ at the nearest bond distance are the same, and we can define a mixed concentration $c_{\mathrm{Ca,Sr}} = 0.2$ and scattering length $\bar{b}_{\mathrm{Ca,Sr}} = 5.86$ fm.

We note that, in the first and second shells of neighbours for the **A** site cations in the perovskite structure, there is a complete overlap of pair distribution functions for **A**$\cdots$**A**, Ti$\cdots$ Ti and O$\cdots$ O. Thus changes in the **A**$\cdots$**A** pair distribution function will, to some extent, be masked in the $D(r)$ data by the contributions from the Ti$\cdots$ Ti and O$\cdots$ O pair distribution functions. Here we quantify the size of the effect.

We note here that we can replace $c_j g_{jj}(r)$ by the values 6 and 12 for the first and second neighbours respectively, and we focus on the sums $S_n = \sum_{ij} c_i c_j \bar{b}_i \bar{b}_j g_{ij}(r_n)$ for the nth neighbour shells. Thus we obtain the following:

$$S_1^{\mathrm{Disordered}} = 176.51 \text{ fm}$$
$$S_1^{\mathrm{Ordered}} = 174.90 \text{ fm}$$
$$S_2^{\mathrm{Disordered}} = 353.02 \text{ fm}$$
$$S_2^{\mathrm{Ordered}} = 356.25 \text{ fm}$$

from which it can be seen that at the first shell the ordering lowers the value of $D(r)$ by around 1%, and at the second shell the ordering raises the value of $D(r)$ by around 1%. These pairs will be repeated throughout the various shells of $D(r)$. This is the size of the effect within the experimental data for $D(r)$ that will drive ordering within the RMC configurations.

Appendix B. Constraints on bond probabilities and local coordination

In this appendix we identify, for reader reference, the constraints on local bond probabilities. For a system containing Ca_xSr_{1-x} cations, where x defines the fraction of atoms that are Ca, we write the probability of a particular bond type as p, and note the following constraints:

$$p_{\mathrm{Ca-Ca}} + 2p_{\mathrm{Ca-Sr}} + p_{\mathrm{Sr-Sr}} = 1$$
$$p_{\mathrm{Ca-Ca}} + p_{\mathrm{Ca-Sr}} = x$$
$$p_{\mathrm{Ca-Sr}} + p_{\mathrm{Sr-Sr}} = 1 - x.$$

(Note that $p_{\mathrm{Sr-Ca}} = p_{\mathrm{Ca-Sr}}$.) It follows that all probabilities are completely correlated, as per

$$p_{\mathrm{Ca-Sr}} = x - p_{\mathrm{Ca-Ca}}$$
$$p_{\mathrm{Sr-Sr}} = 1 - 2x + p_{\mathrm{Ca-Ca}}.$$

Now we consider the coordination numbers as seen by $n(r)$. This function is centred on specific types of atoms with no direct reference to the value of x. Assuming each atom has overall coordination number z, we can write

$$n_{\mathrm{Ca-Ca}} = zp_{\mathrm{Ca-Ca}}/x$$
$$n_{\mathrm{Ca-Sr}} = zp_{\mathrm{Ca-Sr}}/x = z - n_{\mathrm{Ca-Ca}}$$
$$n_{\mathrm{Sr-Sr}} = zp_{\mathrm{Sr-Sr}}/(1-x) = \frac{z}{1-x}(1 - 2x + n_{\mathrm{Ca-Ca}})$$
$$n_{\mathrm{Sr-Ca}} = zp_{\mathrm{Sr-Ca}}/(1-x) = z - n_{\mathrm{Sr-Sr}}.$$

Finally, we define the Warren–Cowley order parameter for any set of neighbouring sites as

$$\alpha = 1 - 2 \times p_{\mathrm{Ca-Sr}}/(1-x) \tag{B.1}$$

where $-x/(1-x) \leqslant \alpha \leqslant 1$ for $x < 0.5$ and $-(1-x)/x \leqslant \alpha \leqslant 1$ for $x > 0.5$. In the case of $x = 0.5$, $\alpha = 0$ for complete disorder, $\alpha = 1$ for complete ordering with neighbouring sites being occupied by the same atom types, and $\alpha = -1$ for complete ordering with neighbouring sites being occupied by different atom types.

These equations are used in tables 1 and 2.

References

[1] Carpenter M A, Howard C J, Knight K S and Zhang Z 2006 Structural relationships and a phase diagram for (Ca, Sr) TiO_3 perovskites *J. Phys.: Condens. Matter* **18** 10725–49

[2] Redfern S A T 1996 High-temperature structural phase transitions in perovskite ($CaTiO_3$) *J. Phys.: Condens. Matter* **8** 8267–75

[3] Ali R and Yashima M 2005 Space group and crystal structure of the perovskite $CaTiO_3$ from 296 to 1720 K *J. Solid State Chem.* **178** 2867–72

[4] Tucker M G, Keen D A, Dove M T, Goodwin A L and Hui Q 2007 RMCProfile: reverse Monte Carlo for polycrystalline materials *J. Phys.: Condens. Matter* **19** 335218

[5] Mellergard A and McGreevy R L 2000 Recent developments of the rmcpow method for structural modelling *Chem. Phys.* **261** 267–74

[6] Proffen Th and Neder R B 1997 DISCUS a program for diffuse scattering and defect structure simulations *J. Appl. Crystallogr.* **30** 171–5

[7] Proffen Th and Welberry T R 1997 Analysis of diffuse scattering via reverse Monte Carlo technique: a systematic investigation *Acta Crystallogr.* A **53** 202–16

[8] Proffen Th and Welberry T R 1998 Analysis of diffuse scattering from single crystals via reverse Monte Carlo technique: II. The defect structure of calcium stabilised zirconia *J. Appl. Crystallogr.* **31** 318–26

[9] Proffen Th 2000 Analysis of occupational and displacive disorder using the atomic pair distribution function: a systematic investigation *Z. Kristallogr.* **215** 661–8

[10] Proffen Th, Petkov V, Billinge S J L and Vogt T 2002 Chemical short range order obtained from the atomic pair distribution function *Z. Kristallogr.* **217** 47–50

[11] Hannon A C 2005 *Nucl. Instrum. Methods Phys. Res.* A **551** 88–107

[12] Dove M T, Tucker M G and Keen D A 2002 *Eur. J. Mineral.* **14** 331–48

[13] Larson A C and Von Dreele R B 1985–2000 *General Structure Analysis System Manual* The Regents of the University of California, Copyright

[14] Toby B H 2001 EXPGUI, a graphical user interface for GSAS *J. Appl. Crystallogr.* **34** 210–21

[15] Tucker M G, Dove M T and Keen D A 2001 Application of the reverse Monte Carlo method to crystalline materials *J. Appl. Crystallogr.* **34** 630–8